Supporting information for

Spontaneous assembly of a class of small molecule prodrugs directed by SN38

Zhenhai Tang,[a] Wenning Lan,[a] Kaiying Wen,[a] Wenting Li,[a] Tao Wang,[b*] Dongdong Zhou,[a*] and Hao Su[a*]

[a]College of Polymer Science and Engineering, State Key Laboratory of Polymer Materials Engineering, Sichuan University, Chengdu 610065, China

[b]Department of Pediatrics, West China Second University Hospital, Sichuan University. No. 20, 3rd section, South Renmin Road, Chengdu 610041, China.

*Corresponding author: hsu@scu.edu.cn; zhoudd@scu.edu.cn; wangtao2001@scu.edu.cn

1. Experimental Section

1.1 Materials

The following chemicals are used as received: 2-Hydroxy-1-ethanethiol (Adamas, > 99%), 2,2′-Dipyridyl disulfide (Adamas, > 99%), 4-dimethylamino pyridine (Adamas, > 99%), 7-Ethyl-10-hydroxycamptothecin (Innochem, > 99%), Pentaethylene glycol monomethyl ether (Innochem, > 98%), Triphosgene (Adamas, > 99%), 4-Nitrobenzoyl chloride (Adamas, > 95%), Di-Tert-Butyl Dicarbonate (Adamas, > 99%), Triethylamine (Greagent, > 99%), 6-Aminohexane-1-Thiol Hydrochloride (Adamas, > 99%), 8-Mercaptooctanoic Acid (Adamas, > 99%), L(+)-Cysteine (Adamas, > 99%), Monothioglycerol (Adamas, > 99%), Triphenylmethyl Chloride (Adamas, > 99%), 2,2,5-Trimethyl-1,3-dioxane-5-carboxylic Acid (Adamas, > 99%), N, N-diisopropylcarbodiimide (Adamas, > 99%), Triisopropylsilane (Adamas, > 99%), Trifluoroacetate (TFA, Adamas, > 99%), Fetal Bovine Serum (FBS, GIBCO), Phosphate Buffer Saline (PBS, pH 7.2, GIBCO), petri dishes (Bkmam Biotechnology Co., Ltd.). All of the solvents were obtained by OKINNO (Cheng du, China). Anhydrous dichloromethane (CH_2Cl_2) was purchased by Adamas (Chengdu, China). OEG_4-SH, OEG_7-SH and OEG_{11}-SH were bought from Biomatrik Inc. (Zhejiang, China).

1.2 Synthesis of SAPDs

1.2.1 Synthesis of Pyr-SS-NO_2

2-Hydroxy-1-ethanethiol (8 g, 102.39 mmol) was dissolved in MeOH (40 mL) and slowly dropped into the solution of 2,2′-Dipyridyl disulfide (45 g, 204.25 mmol) in MeOH (150 mL). The reaction mixture was stirred overnight at room temperature. After the removal of solvent, the crude product was purified by column chromatography using PE/EA (1/1) as eluent to give the pure material (Pyr-SS-OH, pale-yellow oil, 10 g, 52%). MS (ESI-MS) m/z: $[M+H]^+$ calculated for $C_7H_9NOS_2$, 187.0; found 188.1.

Pyr-SS-OH (2.00 g, 10.69 mmol), 4-dimethylamino pyridine (DMAP, 1.3 g, 10.69 mmol) and 4-Nitrobenzoyl chloride (3.22 g, 16.04 mmol) were mixed together in dry DCM (50 mL) and then stirred at room temperature overnight. The reaction mixture was evaporated to remove the solvent and the residue was further purified by chromatography on silica gel with EA/PE (3/7) as the eluent to obtain the Pyr-SS-NO_2 (colorless oil, 2.8 g, 74%). MS (ESI-MS) m/z: $[M+H]^+$ calculated for $C_{14}H_{12}N_2O_5S_2$, 352.0; found 353.0.

1.2.2 Synthesis of Boc-SN38

SN38 (1 g, 2.55 mmol) was suspended in the mixed solution of Di-tert-butyl dicarbonate (0.72 g, 3.3 mmol) and triethylamine (0.52 g, 5 mmol) in DCM (40 mL). After stirred at room temperature for 48 h, the resulting mixture was washed three times with 0.5 M HCl (40 mL) and brine (40 mL), then dried using anhydrous sodium sulfate to obtain BOC-SN38 (pale-yellow solid, 1.02 g, 92%). MS (ESI-MS) m/z: $[M+H]^+$ calculated for $C_{34}H_{42}N_2O_{12}$, 492.2; found, 493.2.

1.2.3 Synthesis of SN38-SS-Pyr

BOC-SN38 (1 g, 2 mmol), Pyr-SS-NO_2 (1.07 g, 3 mmol) and DMAP (0.25 g, 1 mmol) were dissolved in DCM (30 mL). The reaction mixture was heated at 55 ℃ and stirred overnight. The yellow solution was concentrated in vacuo and the residue was further purified by column chromatography with DCM/EA (1/1) as the eluent to give the pure product (Boc-SN38-SS-Pyr, pale-yellow solid, 1.1 g, 77%). MS (ESI-MS) m/z: $[M+H]^+$ calculated for $C_{35}H_{35}N_3O_9S_2$, 705.2; found 706.2.

Trifluoroacetic acid (TFA, 3.21 g, 28.2 mmol) was added dropwise to a solution of Boc-SN38-SS-Pyr (1 g, 1.4 mmol) in DCM (2 mL). The resulting mixture was washed with a saturated solution of $NaHCO_3$ and dried over anhydrous sodium sulfate. The mixture was concentrated in vacuo to obtain the SN38-SS-Pyr (bright yellow powder, 0.75 g, 87.2%). MS (ESI-MS) m/z: $[M+H]^+$ calculated for $C_{30}H_{27}N_3O_7S_2$, 605.1; found 606.2. ^1H NMR (400 MHz, Chloroform-d) δ 8.35 (dt, 1H), 7.99 (d, 1H), 7.59 (dd, 2H), 7.37 (dd, 1H), 7.18 (s, 2H), 6.99 (h, 1H), 5.64 (d, 1H), 5.32 (d, 1H), 4.99 (s, 2H), 4.35 – 4.18 (m, 2H), 2.98 (t, 2H), 2.92 (d, 2H), 2.23 – 2.05 (m, 2H), 1.23 (t, 3H), 0.93 (t, 3H).

1.2.4 Synthesis of SAPD1, SAPD2, and SAPD5

OEG_7-SH (28.06 mg, 78.82 μmol)/OEG_{11}-SH (41.93 mg, 78.82 μmol)/OEG_4-SH (17.65 mg, 78.82 μmol) was dissolved in an N_2-purged DMSO solution SN38-SS-Pyr (40 mg in 2 mL, 65.68 μmol) and shaken overnight. The reaction was diluted to 9 mL with H2O to obtain a slightly viscous solution, which was then purified by RP-HPLC. Product fractions were combined and immediately lyophilized. SAPD1 (pale-yellow solid, 42.1 mg, 75%). MS (ESI-MS) m/z: $[M+H]^+$ calculated for $C_{40}H_{54}N_2O_{14}S_2$, 850.3; found 851.3. SAPD2 (pale-yellow solid, 39.3 mg, 58%). MS (ESI-MS) m/z: $[M+H+Na]^{2+}$ calculated for $C_{48}H_{70}N_2O_{18}S_2$, 1026.4; found 523.0. SAPD5 (pale-yellow solid, 37.9 mg, 80%). MS (ESI-MS) m/z: $[M+H]^+$ calculated for $C_{34}H_{42}N_2O_{11}S_2$, 718.2; found 719.2.

1.2.5 Synthesis of SAPD3/SAPD4

SN38-SS-Pyr (40 mg, 65.68 μmol) was dissolved in an N_2-purged DMSO solution (1 mL) of 6-Aminohexane-1-Thiol Hydrochloride (10.48 mg, 78.82 μmol)/8-Mercaptooctanoic Acid (13.87 mg, 78.82 μmol) and allowed to react overnight. The solution was diluted to 8 mL with H_2O and ACN and purified by RP-HPLC. Product fractions were combined and immediately lyophilized. SAPD3 (pale-yellow solid, 29.3 mg, 71%). MS (ESI-MS) m/z: $[M+H]^+$ calculated for $C_{31}H_{37}N_3O_7S_2$, 627.2; found 628.2. SAPD4 (pale-yellow solid, 30.1 mg, 68%). MS (ESI-MS) m/z: $[M+H]^+$ calculated for $C_{33}H_{38}N_2O_9S_2$, 670.2; found 671.1.

1.3 Characterization of SNPDs

1.3.1 Transmission electron microscopy (TEM)

SAPDs were dissolved in ultrapure water at concentrations of 1 mM and aged overnight at room temperature. The TEM samples were prepared by dropping 6 μL solution onto the grids (300 square mesh) and being wicked by filter paper.[1] The samples were negatively stained by uranyl acetate (20 mg/mL in water), and the procedures were similar to the previous step. The grids were dried at room temperature overnight before TEM imaging (Talos FEI 200i, Thermo

Scientific, USA). The bright-field TEM imaging was obtained at an acceleration voltage of 200 kV.

1.3.2 Circular dichroism (CD) spectroscopy

Stock solutions were prepared at 1mM and aged overnight. All of SAPDs' solution was diluted onsite to 200 μM instantly before measurements, using a 1 mm path length high precision cell (Hellma Analytics) and recording from 190 nm to 450 nm with a 2 nm bandwidth. A mean value of three measurements was used and a pure water background was subtracted to obtain the final result. The final spectra were normalized to the actual concentration of each sample.[2]

1.3.3 Critical micelle concentration (CMC)

Dynamic light scattering (DLS) was commonly utilized to determine the value of CMC.[3] The value of the count rate will undergo a mutation as the free small molecules start to aggregate. Stock solutions were prepared at 1 mM, and diluted to 50, 20, 10, 5, 2, 1, 0.5, 0.2, and 0.1 μM. After aging overnight, the solutions were loaded into a 10 mm path-length Marvin colorimetric dish, and the value of the count rate was recorded by DLS (Malvern Nano ZS ZEN3690). The obtained count rates were plotted as a function of the concentration, which shows a transition in the data when the concentration exceeded the CMC.

1.3.4 Zeta potential measurement

The zeta potential of the assembled structures was measured by observing the electrophoretic motion of the nanostructures in an electric field. The motion speed was determined using phase-analytical light scattering. All SAPDs were dissolved in ultrapure water at a concentration of 1 mM and then aged overnight. The solutions were diluted onsite to 200 μM immediately before measurements and loaded into a folded capillary cell (DTS1070). The zeta potential values were recorded using a Zetasizer Nano ZS ZEN3690. Each SAPD was measured three times, and the average values are shown in **Figure S17**.

1.3.5 *In vitro* drug release

Briefly, a 400 μM solution of SAPDs in deionized water was freshly prepared and allowed to age at room temperature for 24 h. Afterward, it was diluted to 200 μM with PBS (20 mM), with or without GSH (20 mM), at the beginning of the experiment. The solutions were incubated at 37 °C and sampled at 0, 10 min, 20 min, 30 min, 50 min, 1 h, 2 h, 4 h, 8 h, 12 h, and 24 h. For each collected sample, the reductive release was halted by acidification of the solution through the addition of 0.2 μL of 2 M HCl. The samples were flash frozen with liquid nitrogen and stored at -20 °C until HPLC could be performed. The concentration of the residue ratio is determined by measuring the ratio of the area of the HPLC chromatographic peak to the initial peak area.

1.3.6 Cell culture

Colorectal cancer cells (CT26 and HT-29) were kindly provided by Prof. Haoxing Wu (Sichuan University). CT26 was grown in a complete DMEM medium, containing 10% Fetal Bovine Serum (FBS) and 1% of antibiotics. HT-29 was grown in a complete Macoy's medium,

containing 10% FBS and 1% of antibiotics. Both cells were incubated in a humidified atmosphere of 5% CO_2 at 37 ℃.

1.3.7 Cytotoxicity protocol

The cytotoxicity was evaluated by CCK-8 assay. HT-29/CT26 cells were seeded onto a 96-well plate (5000 cells/well) and allowed them to adhere overnight. All SAPDs were diluted with fresh medium and incubated with cells immediately to achieve final conjugate concentrations of 1, 10, 100, 1000, 5000, 10000, 50000, and 100000 nM. Cells were also cultured in SN38 with the same concentration gradient of 0.1, 1, 10, 100, 500, 1000, 5000, and 10000 nM, with untreated cells (medium only) as the control group and medium (without cells) as blank control. In addition, irinotecan with concentrations of 100, 1000, 5000, 10000, 50000, 100000, and 500000 nM was used as the second control. After 48 hours of incubation, all of cells were co-incubated with CCK-8 solution at 37°C for 4 h and the absorbance of each well at 450 nm was determined by a microplate reader (Spark, TECAN, Switzerland) after shaken for 15 min. The cell viability was calculated by

$$\frac{(AbsSAPDs - Absblank)}{(Abscontrol - Absblank)} \times 100\%$$

where the AbsSAPDs, Absblack, and Abscontrol are the absorbance of the SAPDs-treated cells, medium, and untreated cells, respectively.

1.3.8 *In vitro* Cellular Uptake

CT26 cells were seeded onto a 24-well plate with a cell density of 1.5×10^5 cells/well and incubated at 37 °C, in 5% CO_2 overnight. 100 μM SAPDs was prepared by adding 100 μL of 1 mM SAPDs stock solution into 900 μL of DMEM cell medium for CT26 cells. CT26 cells were incubated with the cell medium containing 100 μM of SAPDs for 5 h at 37 °C. After removing medium and washing three times with PBS, 200 μL of trypsin was added to CT26 cells and incubated for 2 min at room temperature. 500 μL of DMEM cell medium was added to each well, and cells were resuspended from the bottom of each well, and then transferred into a 1.5 mL EP tube. All cells were centrifuged at 1.5k RPM for 90 s, and the supernatant was removed. 500 μL of cold 1×PBS was added to wash cells and recentrifuged at 1.5k RPM for 90 s. The supernatant was removed, and 300 μL of cold 1×PBS was added to resuspend cells, which were then transferred into a flow-cytometry tube. 3 μL of propidium iodide (PI) dye solution (4 mg/mL) was added to each sample to mark dead cells and incubated for 30 minutes before testing. 10000 live cells were gated, and fluorescence intensity was detected using a flow cytometer (FACS Aria III, BD).

2. Figures

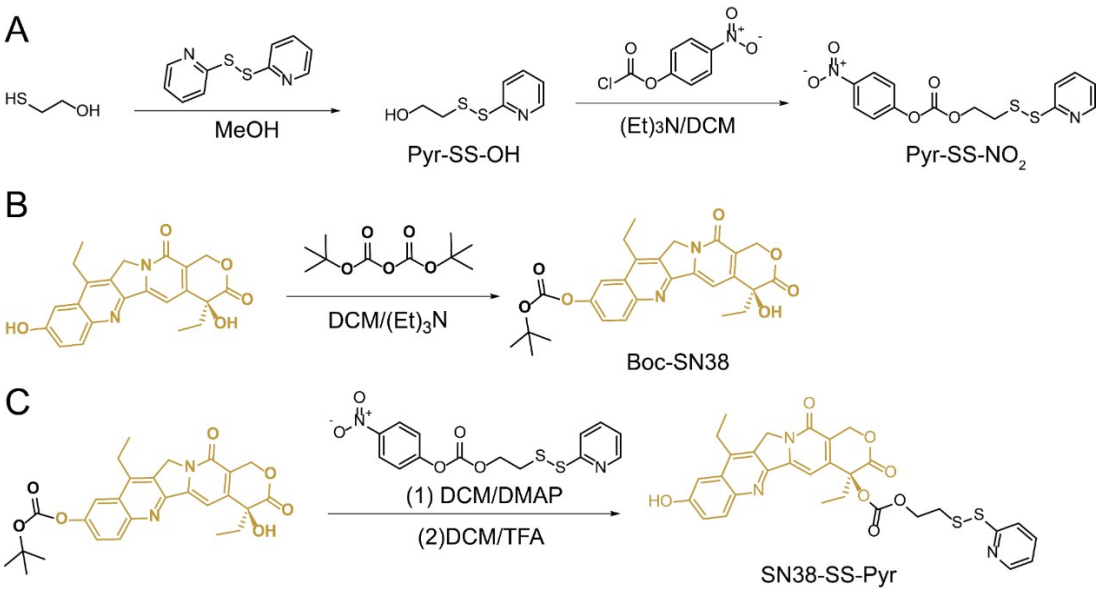

Scheme S1. Synthesis of SN38-SS-Pyr.

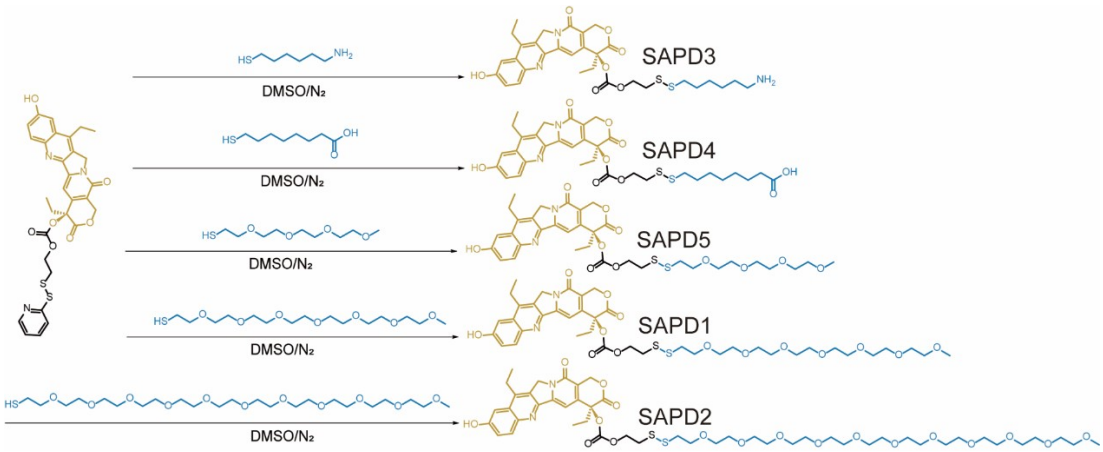

Scheme S2: Synthesis of SAPDs.

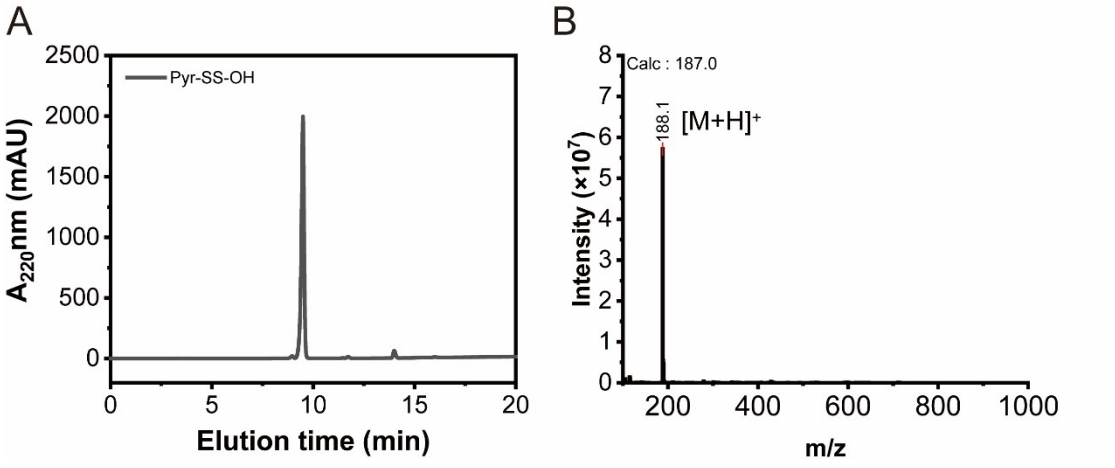

Figure S1. RP-HPLC chromatogram (A) and ESI-MS spectrum (B) of Pyr-SS-OH.

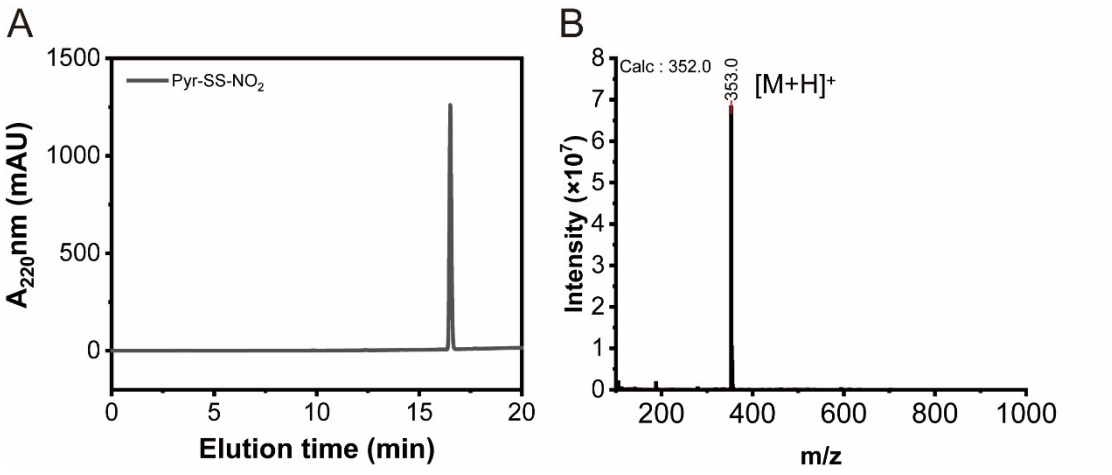

Figure S2. RP-HPLC chromatogram (A) and ESI-MS spectrum (B) of Pyr-SS-NO_2.

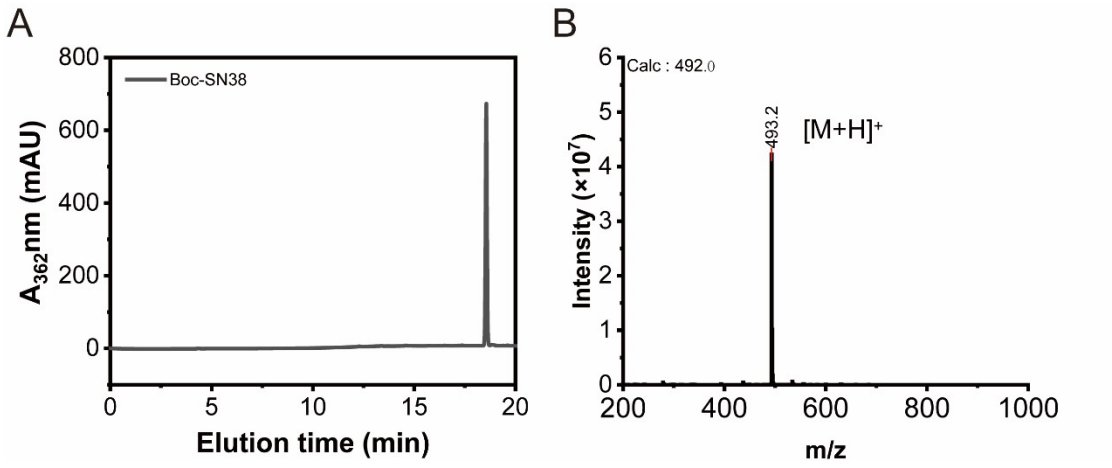

Figure S3. RP-HPLC chromatogram (A) and ESI-MS spectrum (B) of Boc-SN38.

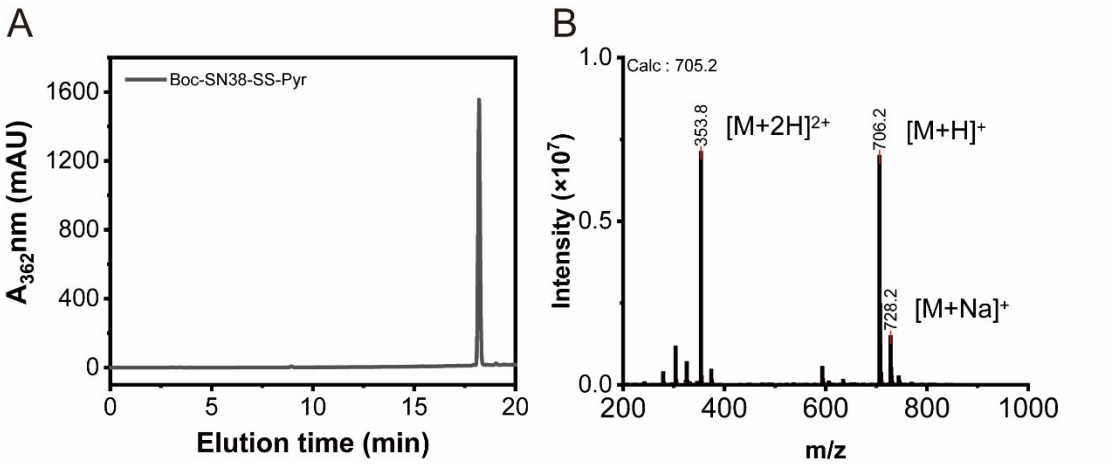

Figure S4. RP-HPLC chromatogram (A) and ESI-MS spectrum (B) of Boc-SN38-SS-Pyr.

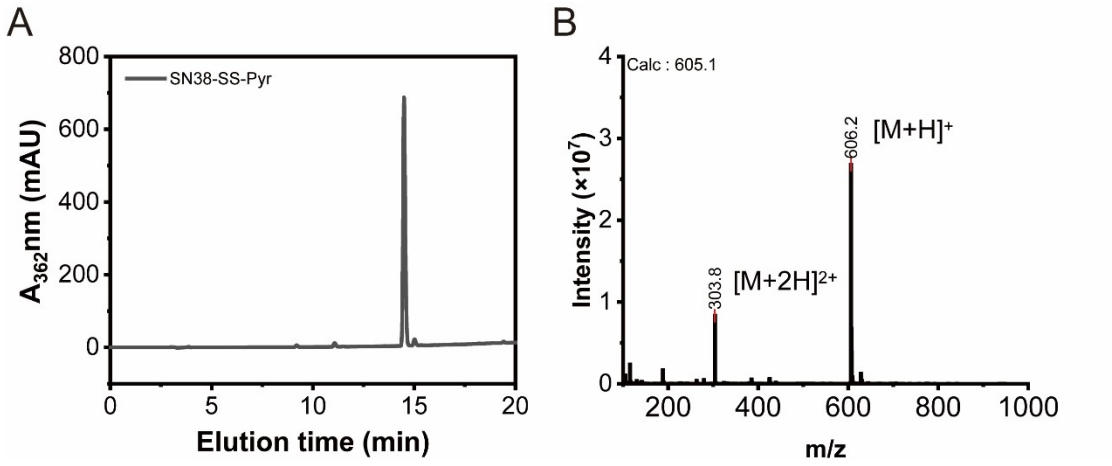

Figure S5. RP-HPLC chromatogram (A) and ESI-MS spectrum (B) of SN38-SS-Pyr.

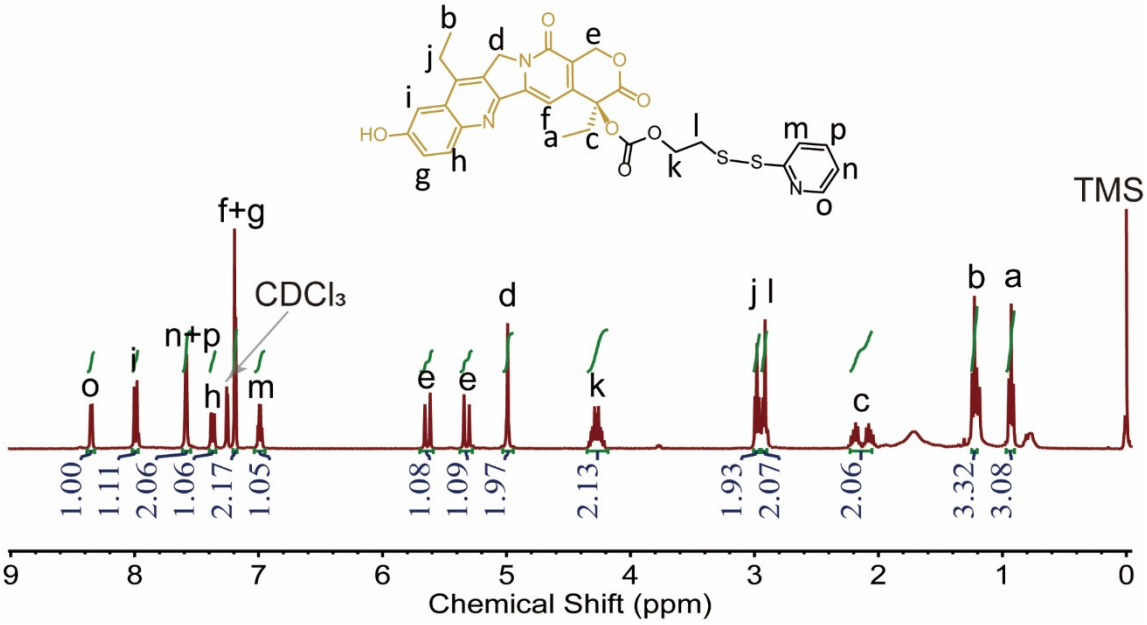

Figure S6. ^{1}H NMR of SN38-SS-Pyr.

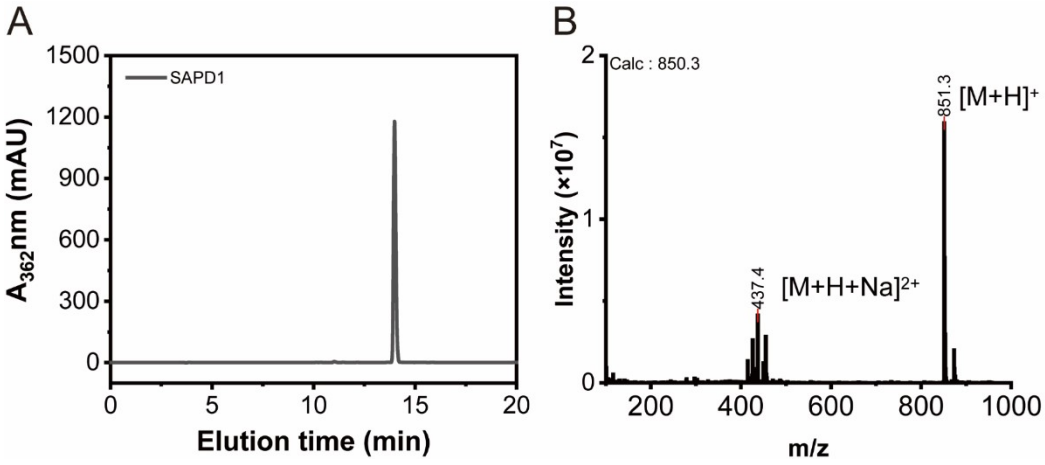

Figure S7. RP-HPLC chromatogram (A) and ESI-MS spectrum (B) of SAPD1.

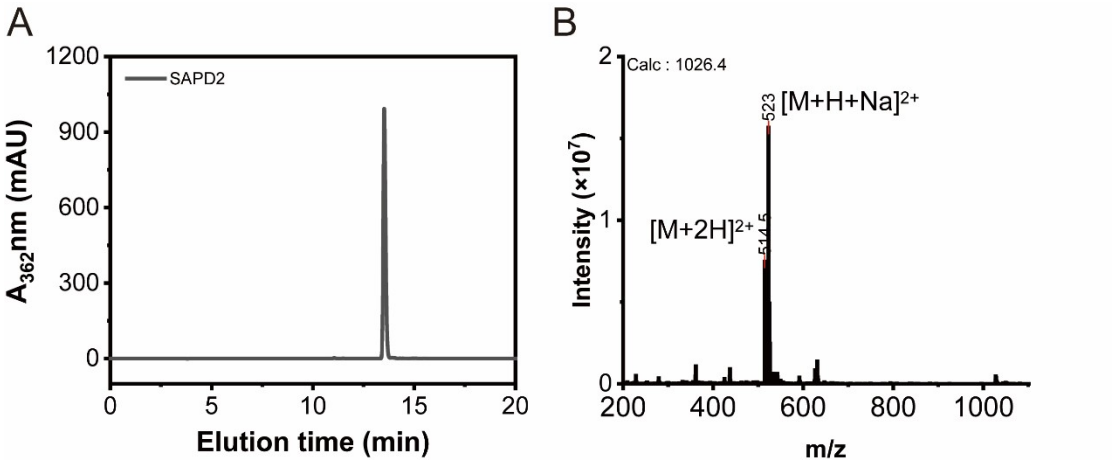

Figure S8. RP-HPLC chromatogram (A) and ESI-MS spectrum (B) of SAPD2.

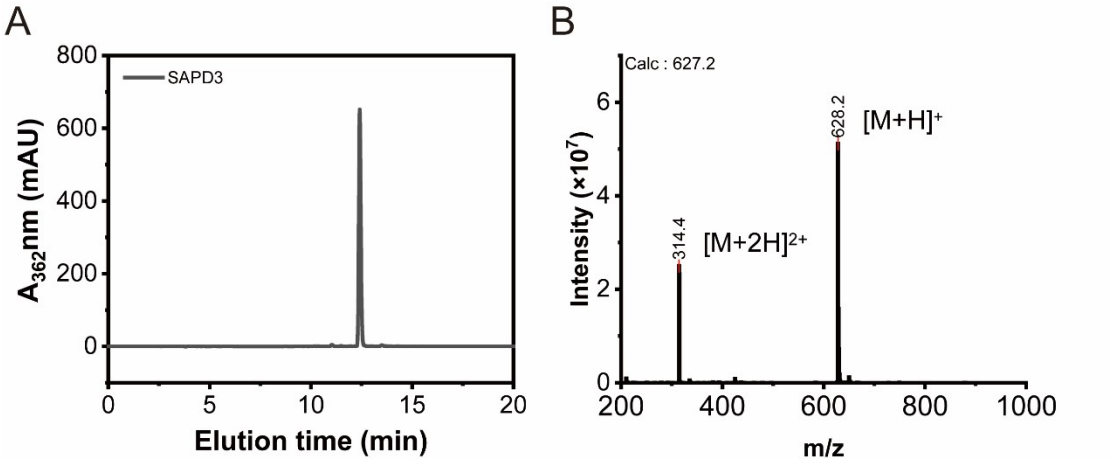

Figure S9. RP-HPLC chromatogram (A) and ESI-MS spectrum (B) of SAPD3.

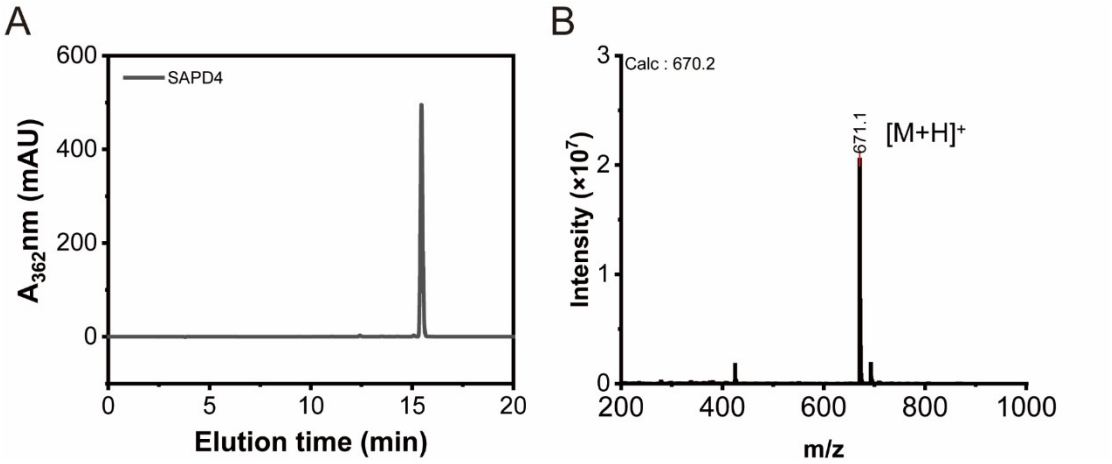

Figure S10. RP-HPLC chromatogram (A) and ESI-MS spectrum (B) of SAPD4.

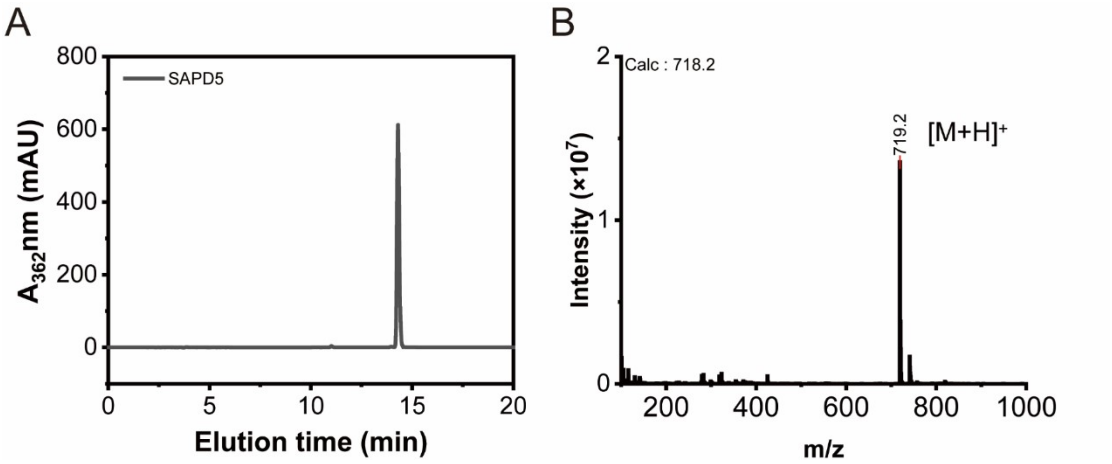

Figure S11. RP-HPLC chromatogram (A) and ESI-MS spectrum (B) of SAPD5.

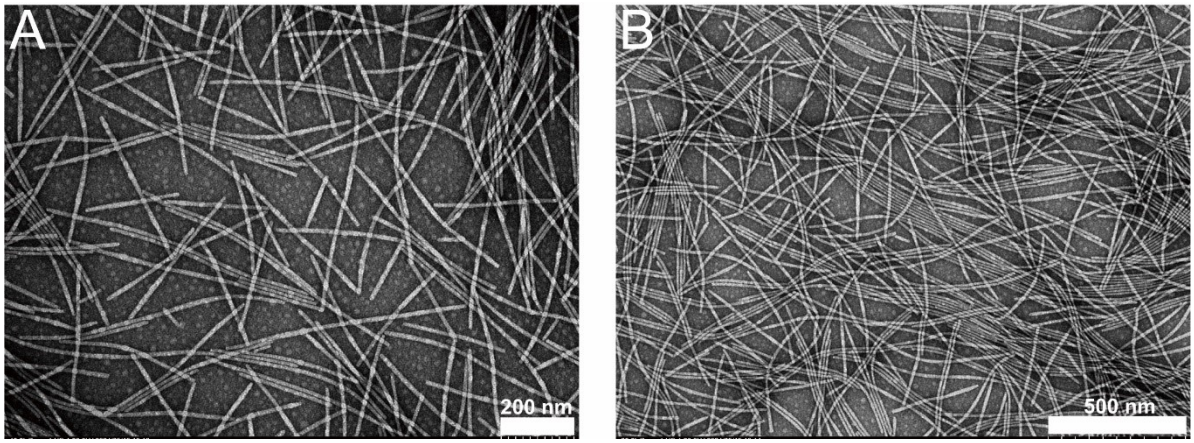

Figure S12. TEM micrographs of SAPD1 at a concentration of 1 mM.

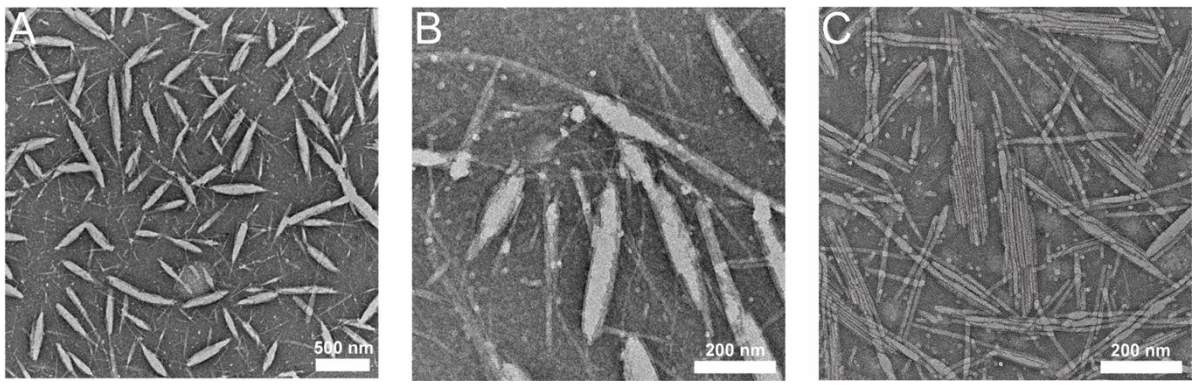

Figure S13. TEM micrographs of SAPD2 at a concentration of 1 mM.

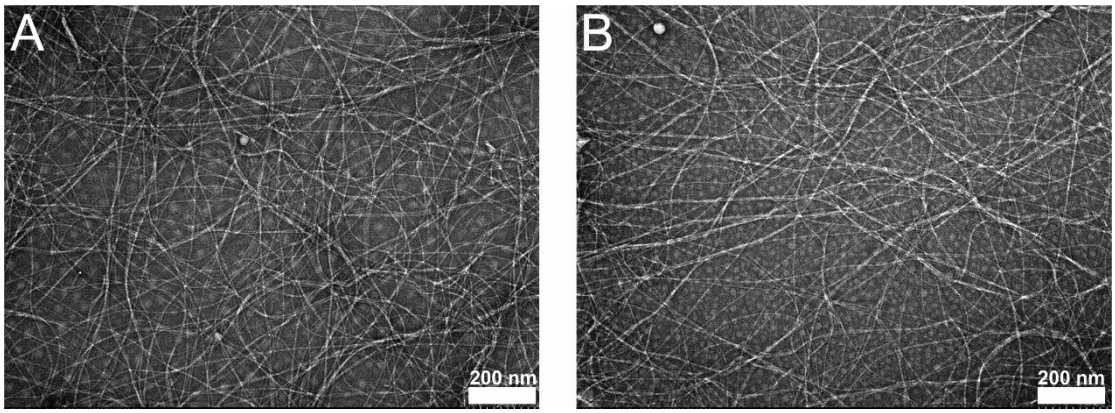

Figure S14. TEM micrographs of SAPD3 at a concentration of 1 mM.

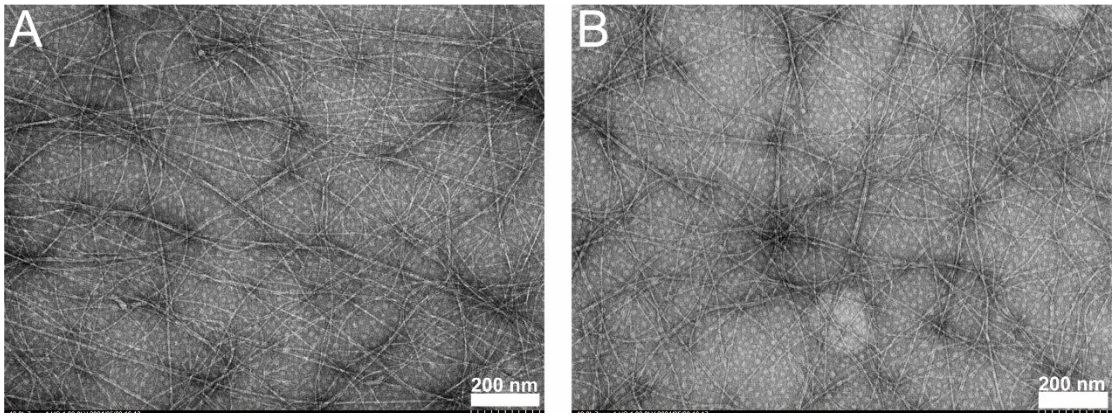

Figure S15. TEM micrographs of SAPD4 at a concentration of 1 mM.

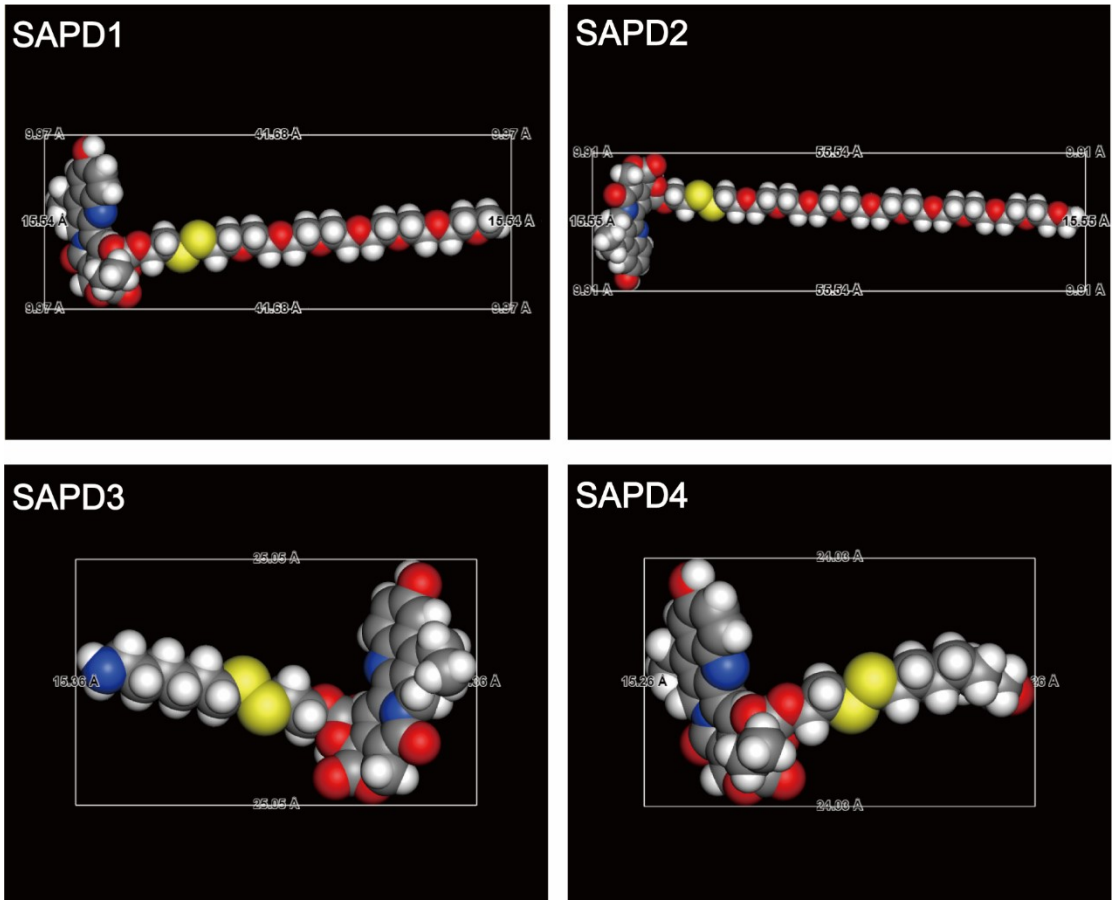

Figure S16. Molecular size of SAPDs.

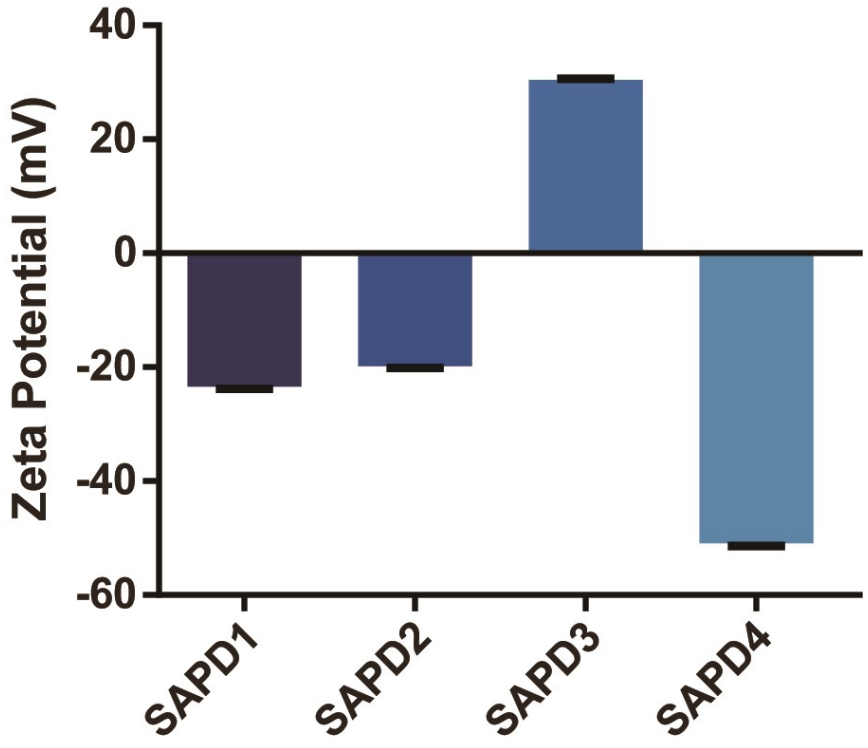

Figure S17. ζ-Potential values of assembled SAPDs in water.

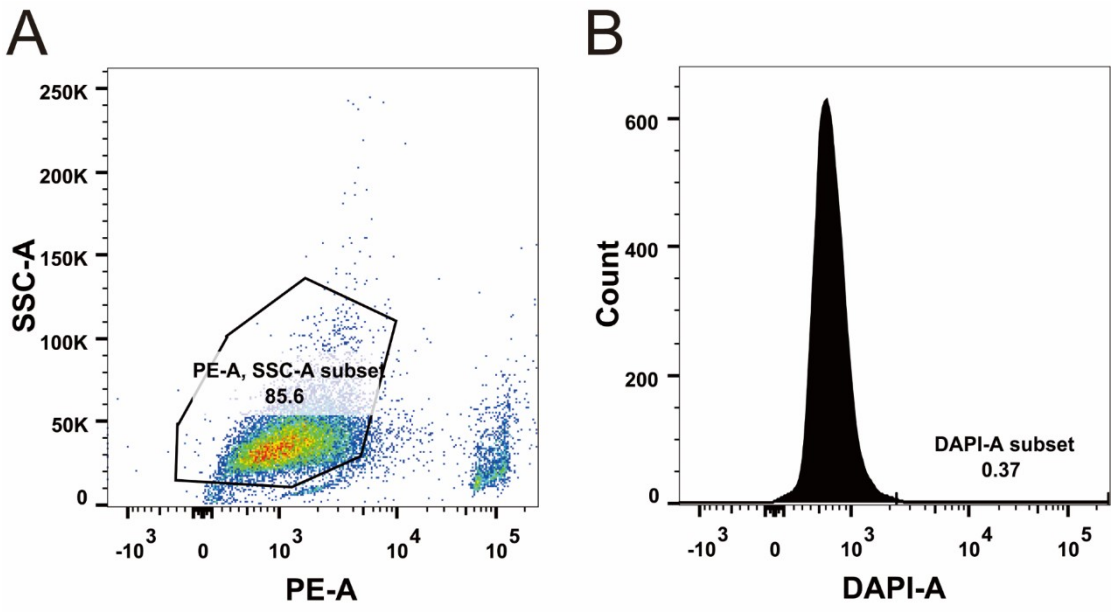

Figure S18. Flow cytometry data from experiments with control cells (no nanofibers added). Double scatter plots of side scattering (y-axis) versus fluorescence intensity distributions (in logarithmic scale on x-axis) (gating live cells) (A), and fluorescence intensity distributions (in logarithmic scale on x-axis) versus cell count (y-axis) following SN38 fluorescence (λex = 355 nm, λem = 450 nm) (B).

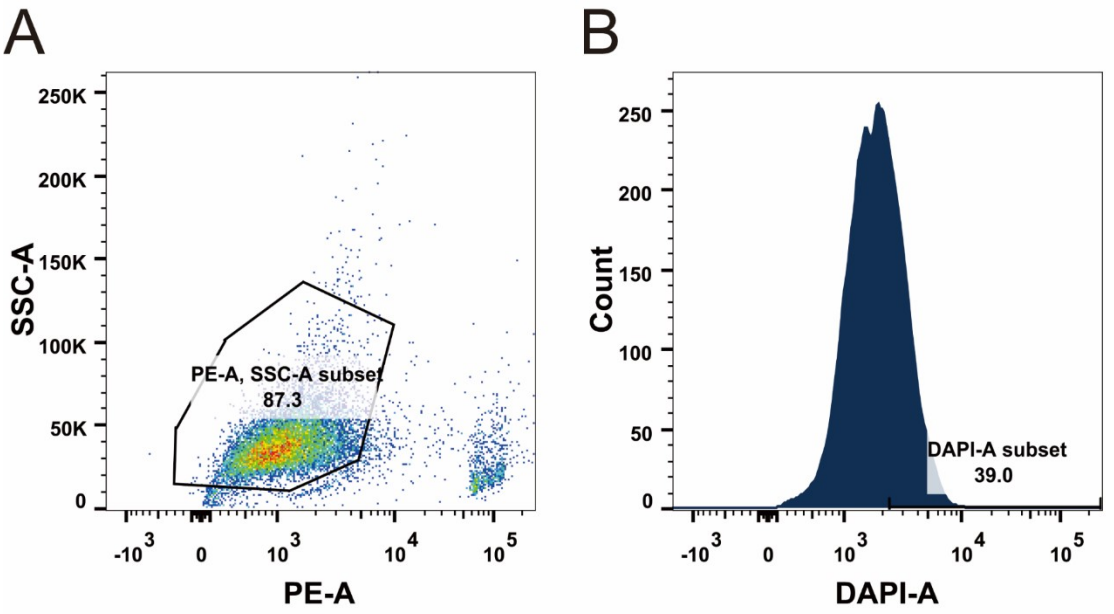

Figure S19. Flow cytometry data from experiments with CT26 cells (treated with SAPD1). Double scatter plots of side scattering (y-axis) versus fluorescence intensity distributions (in logarithmic scale on x-axis) (gating live cells) (A), and fluorescence intensity distributions (in logarithmic scale on x-axis) versus cell count (y-axis) following SN38 fluorescence (λex = 355 nm, λem = 450 nm) (B).

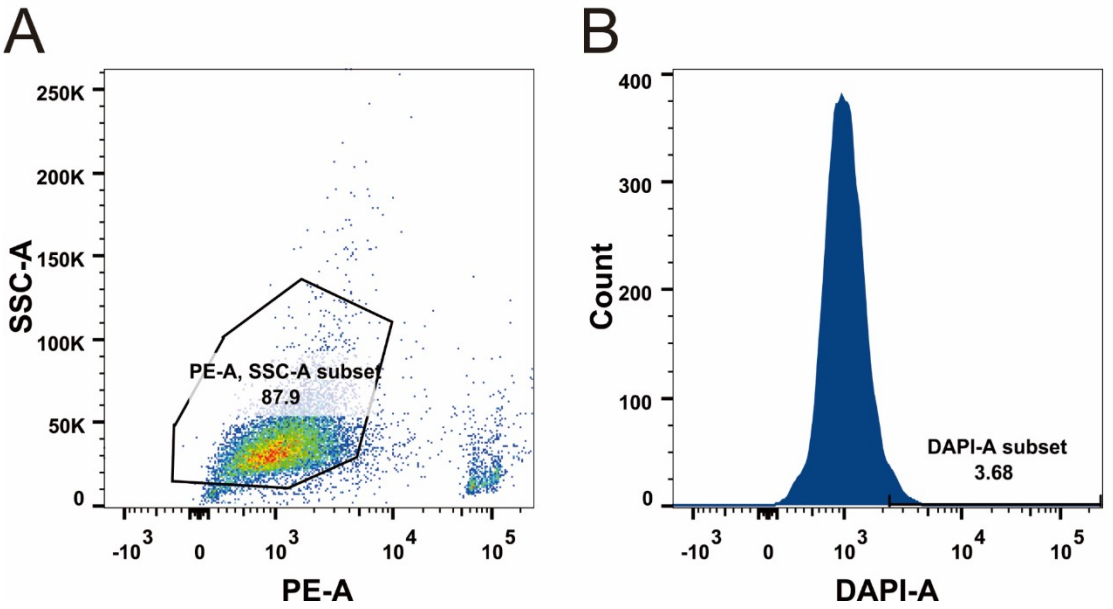

Figure S20. Flow cytometry data from experiments with CT26 cells (treated with SAPD2). Double scatter plots of side scattering (y-axis) versus fluorescence intensity distributions (in logarithmic scale on x-axis) (gating live cells) (A), and fluorescence intensity distributions (in logarithmic scale on x-axis) versus cell count (y-axis) following SN38 fluorescence (λex = 355 nm, λem = 450 nm) (B).

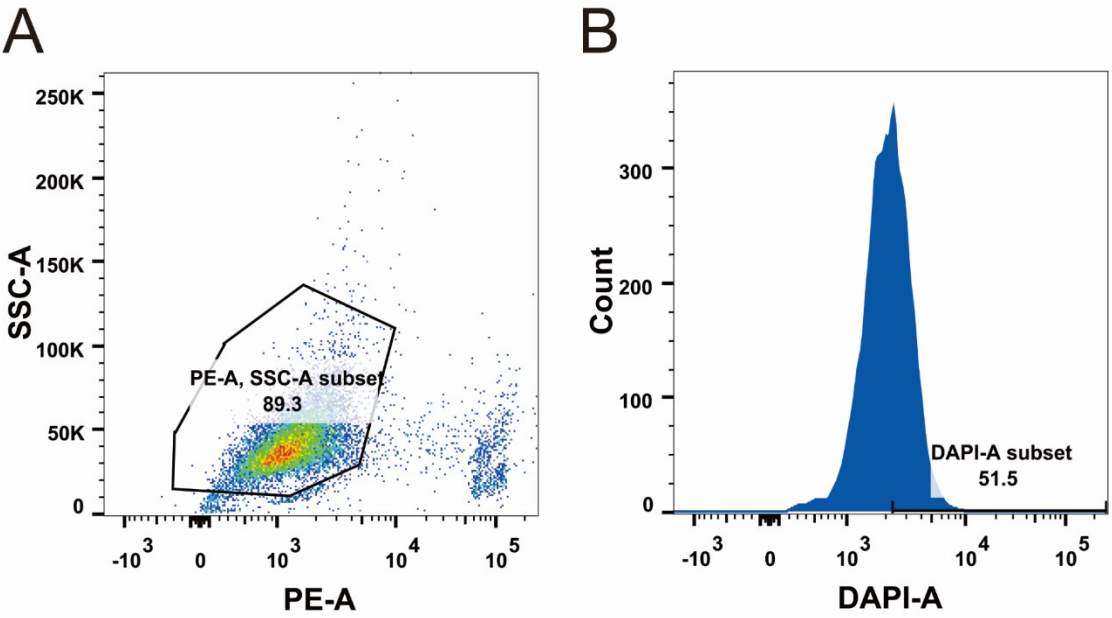

Figure S21. Flow cytometry data from experiments with CT26 cells (treated with SAPD3). Double scatter plots of side scattering (y-axis) versus fluorescence intensity distributions (in logarithmic scale on x-axis) (gating live cells) (A), and fluorescence intensity distributions (in logarithmic scale on x-axis) versus cell count (y-axis) following SN38 fluorescence (λex = 355 nm, λem = 450 nm) (B).

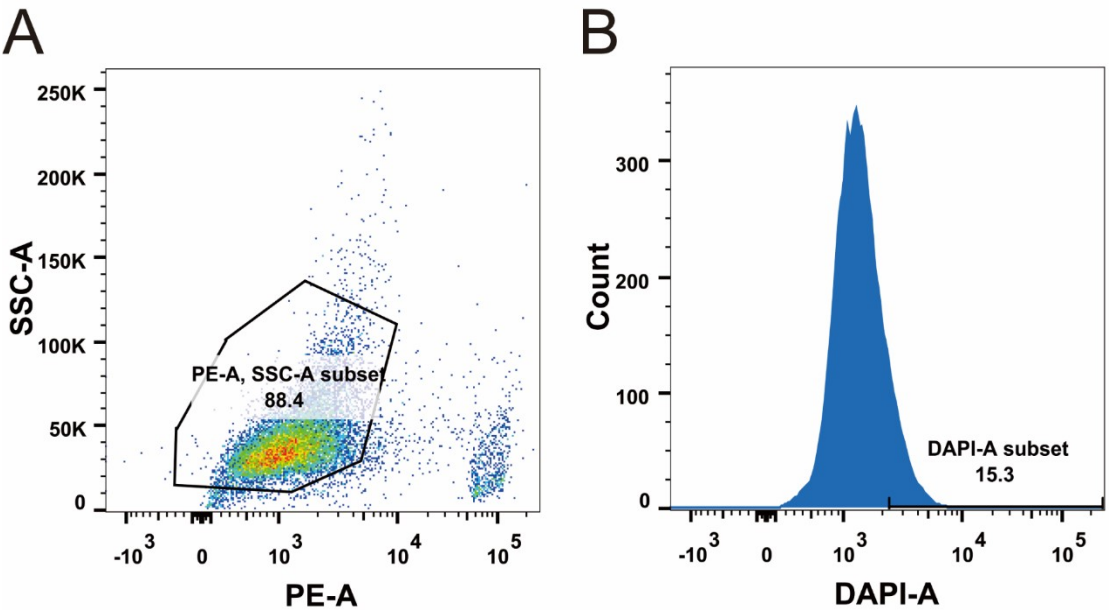

Figure S22. Flow cytometry data from experiments with CT26 cells (treated with SAPD4). Double scatter plots of side scattering (y-axis) versus fluorescence intensity distributions (in logarithmic scale on x-axis) (gating live cells) (A), and fluorescence intensity distributions (in logarithmic scale on x-axis) versus cell count (y-axis) following SN38 fluorescence (λex = 355 nm, λem = 450 nm) (B).

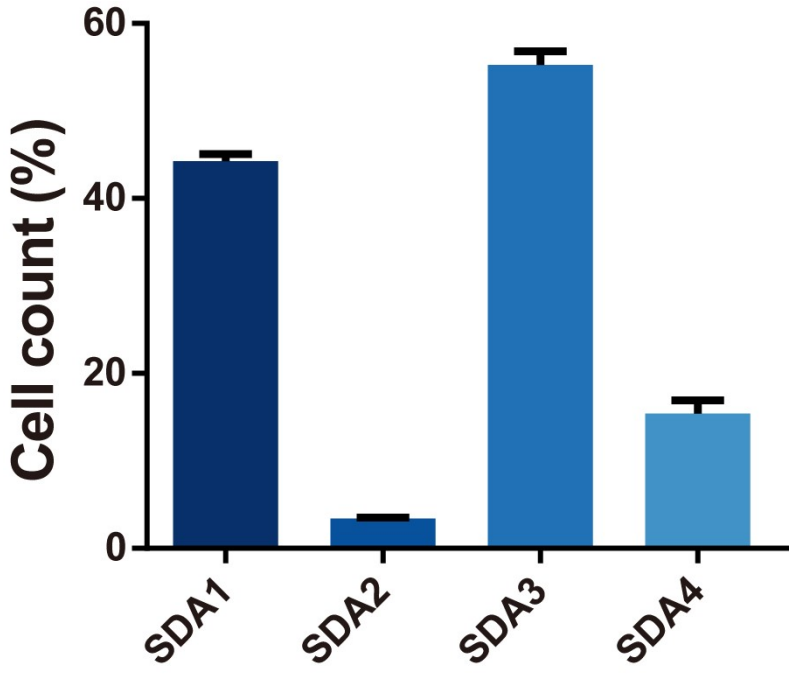

Figure S23. Effect of charge, and shape of SAPDs nanofibers on the cellular uptake efficiency by CT26 cancer cells, characterized using flow cytometry. Cell counting measurement.

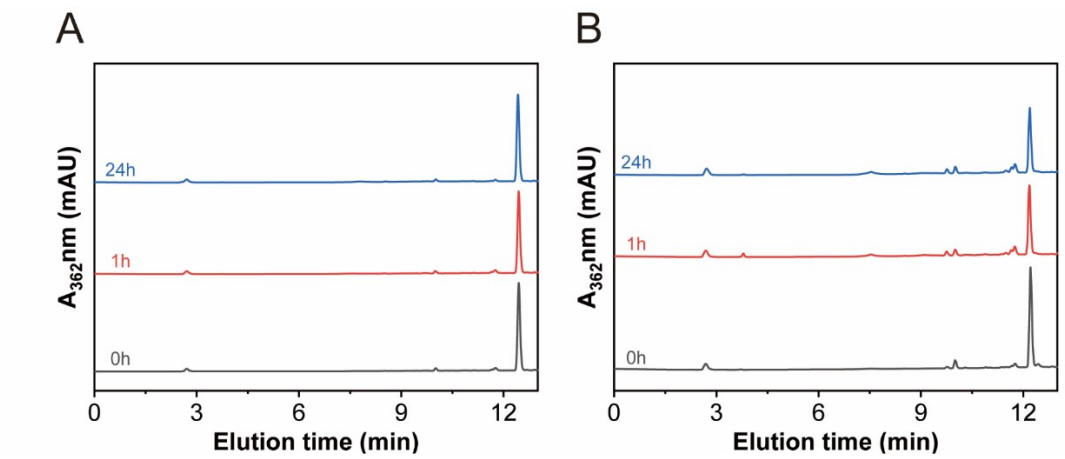

Figure S24. Drug release of SAPDs at 200 μM in PBS without GSH. Comparison of HPLC spectra at different time points: SAPD1 (A) and SAPD2 (B).

References:

(1) Su, H.; Zhang, W.; Wang, H.; Wang, F.; Cui, H. Paclitaxel-Promoted Supramolecular Polymerization of Peptide Conjugates. *J. Am. Chem. Soc.* **2019**, *141* (30), 11997–12004.

(2) Cheetham, A. G.; Zhang, P.; Lin, Y.; Lock, L. L.; Cui, H. Supramolecular Nanostructures Formed by Anticancer Drug Assembly. *J. Am. Chem. Soc.* **2013**, *135* (8), 2907–2910.

(3) Liang, C. H.; Chen, Y. X.; Zheng, D. B.; Xu, T. Y.; Pu, G. J.; Chen, Y. M.; Wang, L.; Yang, Z. M.; Wang, H. M. Pathway-Dependent Supramolecular Polymerization of Camptothecin Derivatives into Filaments for Chemotherapy and Imaging. *Appl. Mater. Today* **2020**, *20*, 100787.